Society For Biomaterials

Modulation of macrophage phenotype via phagocytosis of drug-loaded microparticles

Kathryn L. Wofford,[1,2,3] D. Kacy Cullen,[2,3,4] Kara L. Spiller[1]

[1]School of Biomedical Engineering, Science and Health Systems, Drexel University, Philadelphia, Pennsylvania
[2]Center for Neurotrauma, Neurodegeneration and Restoration, CMC VA Medical Center, Philadelphia, Pennsylvania
[3]Department of Neurosurgery, University of Pennsylvania, Philadelphia, Pennsylvania
[4]Department of Bioengineering, University of Pennsylvania, Philadelphia, Pennsylvania

Received 14 October 2018; accepted 9 January 2019
Published online 00 Month 2019 in Wiley Online Library (wileyonlinelibrary.com). DOI: 10.1002/jbm.a.36617

Abstract: Monocyte-derived macrophages play a critical role in directing wound pathology following injury. Depending on their phenotype, macrophages also promote tissue regeneration. However, the therapeutic administration of macrophages with a controlled phenotype is challenging because macrophages are highly plastic and quickly revert to a detrimental, inflammatory phenotype in response to the environment of a damaged tissue. To address this issue, we developed a novel strategy to modulate macrophage phenotype intracellularly through phagocytosis of drug-loaded microparticles. Poly(lactic-co-glycolic acid) microparticles loaded with the anti-inflammatory drug dexamethasone (Dex) were phagocytosed by monocytes and stored intracellularly for at least 5 days. After differentiation into macrophages, cell phenotype was characterized over time with high-throughput gene expression analysis via NanoString. We found that the microparticles modulated macrophage phenotype for up to 7 days after microparticle uptake, with decreases in inflammation-related genes at early timepoints and upregulation of homing- and phagocytosis-related genes at multiple timepoints in a manner similar to cells treated with continuous free Dex. These data suggest that intracellularly loading macrophages with Dex microparticles via phagocytosis could be a unique methodology to selectively modulate macrophage phenotype over time. This strategy would allow therapeutic administration of macrophages for the treatment of a number of inflammatory disease and disorders. J Biomed Mater Res Part A: 00A: 000–000, 2019.

Key Words: macrophage, intracellular particles, dexamethasone, gene expression, cell–microparticle interactions

How to cite this article: Wofford KL, Cullen DK, Spiller KL. 2019. Modulation of macrophage phenotype via phagocytosis of drug-loaded microparticles. J Biomed Mater Res Part A 2019:00A:1–12.

INTRODUCTION

Prolonged inflammation is a characteristic of many diseases and disorders. Macrophages, the primary innate immune cells of the body, play a large role in directing inflammation within damaged tissues, but they can also promote tissue regeneration.[1–4] Macrophages facilitate tissue regeneration by homing to injured tissue, phagocytosing necrotic and apoptotic debris, and secreting proteins that guide tissue regeneration.[5] Over the last several decades, researchers have explored the plasticity of macrophages and found that macrophages can exhibit a spectrum of activation phenotypes ranging from inflammatory to anti-inflammatory to tumor-suppressive to angiogenic[5,6] (for reviews, see Refs. 1,7). Importantly, it has been hypothesized that controlling macrophage phenotype could redirect non-healing wounds and diseases toward a more regenerative environment and ultimately guide tissue regrowth.[7,8]. However, attempts to overcome chronic inflammation by locally administering anti-inflammatory macrophages into the damaged tissue have been unsuccessful because macrophages rapidly respond to their environment and quickly revert to a detrimental, inflammatory state.[9,10]

Administration of the corticosteroid dexamethasone (Dex) affects macrophage phenotype by inhibiting the expression of genes related to inflammation[11–13] and promoting genes related to homing,[14] phagocytosis,[15–20] and iron metabolism, [21] functions that promote tissue regeneration. However, systemic Dex administration has failed in a number of clinical trials and cannot be tolerated by patients over long treatment regimens because of adverse side effects.[22–26] This is most likely because systemically administered Dex affects a broad population of cells and results in

Additional Supporting Information may be found in the online version of this article.
Correspondence to: K.L. Spiller; e-mail: spiller@drexel.edu
Contract grant sponsor: Department of Veteran's Affairs; contract grant number: I01-RX001097
Contract grant sponsor: National Heart, Lung, and Blood Institute; contract grant number: R01-HL130037
Contract grant sponsor: Department of Education GAANN iCARE Fellowship

non-specific immunosuppression, especially of the adaptive immune system.[27,28]

Clearly, there is a need to develop a strategy to selectively modulate macrophage behavior toward an anti-inflammatory, pro-regeneration phenotype without the detrimental effects of systemic corticosteroid administration. To address these challenges, we postulate that selective delivery of Dex to macrophages may allow control over macrophage behavior without inducing systemic side effects. Accordingly, in the current study we investigated whether Dex, released from intracellular-microparticles, could maintain its bioactivity and downregulate macrophage gene expression related to inflammation and promote macrophage gene expression related to homing, phagocytosis, and iron metabolism. We hypothesized that selectively administering Dex-loaded microparticles to monocyte-derived macrophages will allow the microparticles to be rapidly phagocytosed, where they can intracellularly redirect macrophage phenotype.

To test this hypothesis, we fabricated poly(lactic-co-glycolic acid) (PLGA) microparticles loaded with two doses of Dex. We cultured the microparticles with human primary monocytes for several hours to allow phagocytosis. Non-phagocytosed microparticles were then washed away and the monocytes were plated and differentiated into macrophages (Fig. 1). RNA was collected over the course of 1 week to characterize the effects of intracellular Dex microparticles on macrophage gene expression (Fig. 1). This experimental paradigm was designed to preserve translational treatment applicability for clinical patients. Because monocytes are easily accessible – they can be isolated from patients in the clinic with a simple blood draw – these cells hold great potential to be modulated *ex vivo* with minimal manipulation and re-administered to patients so that they can home to damaged tissues and promote regeneration.

MATERIALS AND METHODS

Microparticle fabrication

Single emulsion PLGA microparticles were fabricated with or without Dex. Briefly, 20 mg/mL of PLGA (cat# 5050DLG4A from Evonik) was suspended in a 9:1 solution of dichloromethane (DCM) (cat# 364230010 from Acros Organics) to trifluoroethanol (TFE) (cat# T63002 from Sigma-Aldrich). Dex (cat# A17590 from Alfa Aesar) was added into the solution to generate a final concentration of 0, 10, or 25 mg/mL Dex in the organic solution. The solution was mixed via sonication for 30 s on ice. Afterward, the organic solution was added to 2% polyvinyl alcohol (cat# 363170 from Sigma-Aldrich) and allowed to stir at 1200 rpm for 6 h to facilitate organic solvent evaporation and microparticle hardening. After hardening, microparticles were collected via centrifugation, separated from the supernatant, and characterized for microparticle size and polydispersity index via dynamic light scattering on a Malvern Zetasizer. Thereafter, microparticles were lyophilized, resuspended at 1 mg/mL in 1× PBS, and stored at −80°C until use. Microparticles with no Dex are referred to as "blank microparticles", microparticles fabricated with 10 mg/mL Dex in the organic solution are referred to as "low Dex microparticles", and microparticles fabricated with 25 mg/mL Dex in the organic solution are referred to as "high Dex microparticles".

Primary human monocyte cell culture

Human primary monocytes were obtained from the University of Pennsylvania Human Immunology Core. Monocytes were suspended in freezing media (50% RPMI 1640, 40% heat inactivated human serum, and 10% DMSO) at a concentration of 10×10^6 cells/mL and frozen until initiation of the *in vitro* study.

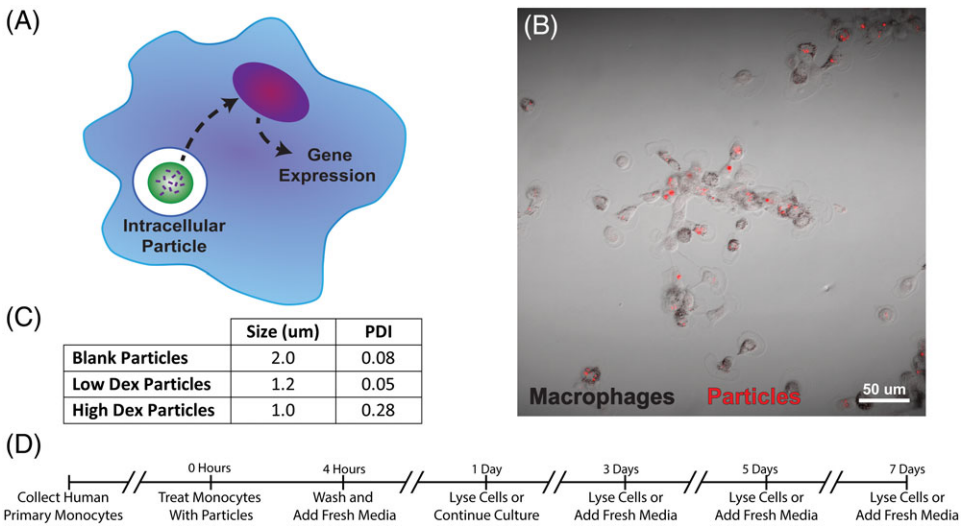

	Size (um)	PDI
Blank Particles	2.0	0.08
Low Dex Particles	1.2	0.05
High Dex Particles	1.0	0.28

FIGURE 1. Overall strategy and experimental design. Genes related to homing, inflammation, phagocytosis, and iron metabolism were analyzed from cells treated with Dex microparticles (A). Microparticles were pre-administered to primary human monocytes on day 0 to facilitate particle uptake. Particles were rapidly phagocytosed by macrophages and were detectable intracellularly for 5 days after administration (B; particles are red). Particle diameter fell between 1.0 and 2.0 μm and polydispersity indices were all less than 0.3 (C). After particle treatment, cells were washed and plated. Cell lysates were collected from macrophages on days 1, 3, 5, and 7 in order to analyze gene expression (D).

Briefly, frozen human primary monocytes were thawed and resuspended at 2×10^6 cells/mL in standard culture media consisting of 89% RPMI 1640, 10% heat inactivated human serum, and 1% Pen/Strep. The cell suspensions were treated with either 20 μg of blank, low, or high Dex microparticles per million cells; 10^{-4} *M* free Dex; or were not supplemented with anything. The human monocytes were incubated in their treatment condition for 4 h while shaking at 100 rpm at 37°C.

After 4 h, the cells were spun down at 400 g for 7 min. The supernatant was removed and cells were resuspended at 1×10^6 cells/mL in standard media supplemented with 20 ng/mL macrophage colony stimulating factor (MCSF). Cells were then seeded in ultra-low attachment plates and incubated at 37°C (n = 5). Thereafter, media was replaced on days 3 and 5 of the experiment. Cells in the free Dex condition always received media supplemented with 10^{-4} *M* Dex. Cells were cultured for either 1, 3, 5, or 7 days before collection for RNA isolation.

Characterization of intracellular microparticles with confocal microscopy

A small batch of PLGA microparticles were fabricated according to the methodology above but the fluorescent marker Nile Red was added into the organic solution to generate a final concentration of 0.4 mg/mL. These microparticles were administered to primary human monocytes and followed the same procedural timeline, except on day 5 the cells were washed and fixed in 10% formaldehyde. Cells were imaged on a Zeiss LSM700 Laser Scanning Confocal to visualize fluorescent intracellular microparticles.

RNA purification

At the designated timepoint, cells were lysed and RNA was isolated according to the manufacturer's instructions from the RNAqueous-Micro Total RNA Isolation Kit (cat# AM1931 from ThermoFisher Scientific) and stored at −80°C until RNA isolation. Briefly, lysis solution was neutralized, and samples were loaded onto a silica filter. Samples were then washed thoroughly, eluted into a small volume, and then quantified for RNA concentration and quality on a ThermoScientific NanoDrop 1000 Spectrophotometer. RNA quality met manufacturer's guidelines and is reported in Supporting Information Fig. 1.

Gene expression quantification

In order to quantify expression of a panel of genes across a large number of samples, we employed a multiplex, high throughput NanoString PlexSet quantification platform. The assay utilizes unique fluorescent probes bound to custom-made oligonucleotides in order to generate absolute counts of gene expression from isolated RNA. We first designed and ordered a set of custom oligonucleotides from Integrated DNA Technologies that were designed to bind to either the reporter probes or capture probes from the NanoString 24-gene PlexSet and to the target RNA from experimental samples (Supporting Information Fig. S2). The oligonucleotides and probes employed were selected to investigate the expression of genes related to macrophage inflammation, homing, phagocytosis, iron metabolism, and housekeeping functions. The NanoString assay was completed according to manufacturer's instructions where the oligonucleotides were added to appropriate Master Mixes containing the unique reporter and capture probes. Thereafter, experimental samples (n = 4 or 5) were added to the solution and allowed to hybridize with the oligonucleotides at 67°C for 21 h and then cooled to 4°C. Following hybridization, samples were processed in the NanoString MAX Prep Station and nCounter machines per the manufacturer's instructions.

Data analysis and statistics

Raw counts of gene expression data were processed according to Nano String's recommendations. Data were preprocessed by subtracting out the negative control for each sample and normalizing to the geometric mean of the positive controls. Afterward, data were normalized to the average of the three housekeeping genes (*LDHA*, *PGK1*, and *RPL19*) in each experimental sample. As expected, the gene expression data for all of the samples were positively skewed. A Box–Cox function with lambda set to 0.15 was applied to transform the data to reach approximate normality (Supporting Information Fig. 3).

Within each gene, data were analyzed with a two-way ANOVA to investigate the significance of the factors: treatment condition, time, and the interaction between treatment condition and time. To investigate differences between treatment conditions at a given time point, data were analyzed with a one-way ANOVA followed by a Tukey's honest significant difference post hoc test. Post hoc p-values were corrected for multiple comparisons, the type I error rate was set to 0.05, and all hypothesis tests were two-sided. To simplify data presentation, all bar and line graphs (Figs. 4–7) were plotted from the data prior to transformation. Importantly, all the statistical analyses were completed on transformed data. All data and statistical analyses were completed in R Studio version 1.0.143 except for the principle component analysis (PCA), which was completed in MATLAB version 2017b (9.3.0.713579).

RESULTS

Microparticle characteristics

Single emulsion PLGA microparticles were fabricated with increasing doses of Dex to generate three groups of microparticles denoted blank microparticles, low Dex microparticles, or high Dex microparticles. PLGA microparticles across Dex dose were all between 1.0 and 2.0 μm in diameter and all microparticle groups contained a polydispersity index of less than 0.4 (Fig. 1C). High Dex microparticles were half the diameter of blank microparticles but all groups were within the size range that is readily phagocytosed by macrophages.[29] Phagocytosed microparticles, fluorescently labeled with Nile Red, were visually detectable intracellularly 5 days after microparticle administration (Fig. 1B).

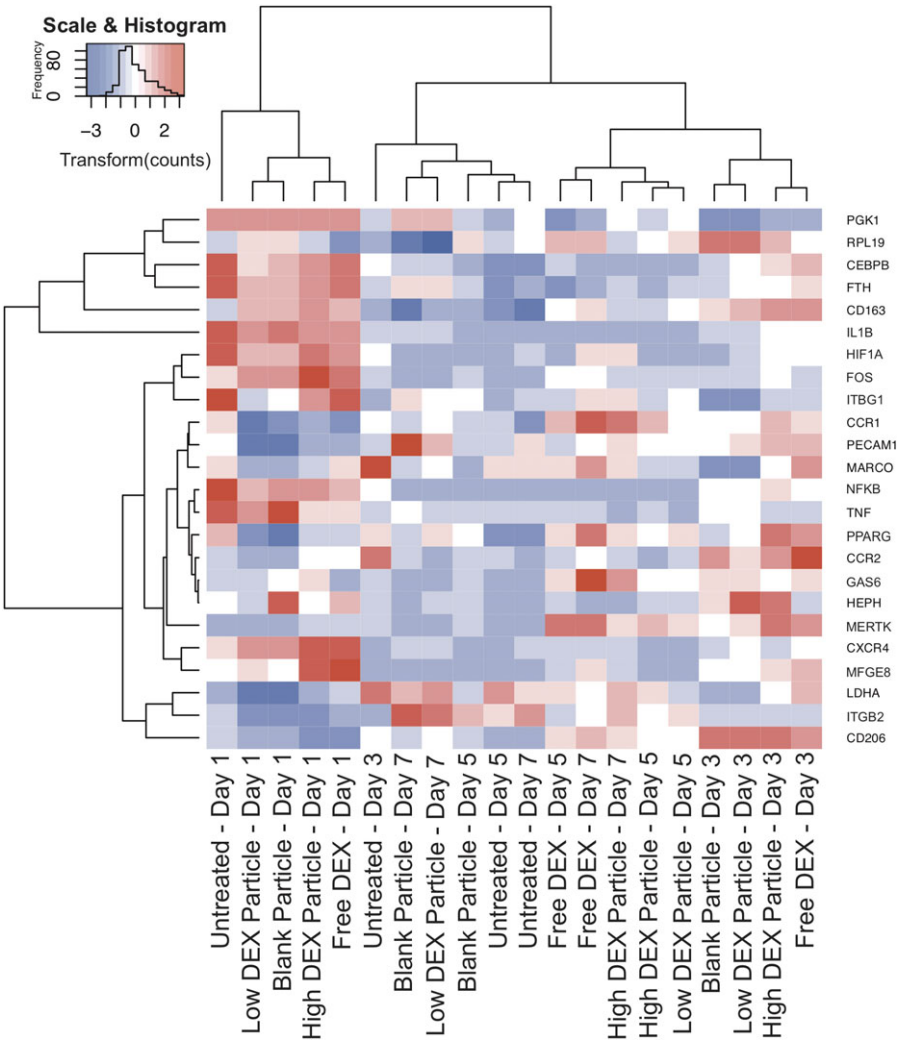

FIGURE 2. Gene expression of macrophages. High-throughput gene expression analysis was quantified with a NanoString PlexSet assay and a custom-designed list of genes related to inflammation, homing, phagocytosis, and iron metabolism. Transformed data were plotted in a heatmap with scaling by rows (genes). Dendrograms on top of the heatmap and to the left of the heatmap represent clustering by sample and clustering by gene, respectively. Blue colors represent lower levels of gene expression and red colors represent higher levels of gene expression.

Gene expression analysis

Global gene analysis trends. To visualize overarching gene expression patterns across samples, we plotted a heatmap and dendrogram across treatment condition and time (columns) against gene expression (rows) (Fig. 2). Dendrogram clustering suggested that the greatest effect on gene expression patterns was due to time. After that, within each time point, the untreated groups generally clustered away from the treatment groups. Furthermore, the cells treated with low Dex microparticles clustered with the untreated cells and the cells treated with blank microparticles, while cells treated with high Dex microparticles generally clustered with the cells treated with continuous free Dex.

These trends were confirmed with PCA, which captured 61.3% of the total variance in the first two principal components (Fig. 3). Notably, separation of the experimental samples by PC1 clearly separated samples by the time they spent in culture. Most notably, cells that were collected on day 1 clustered together and behaved in a distinct way from cells collected at later time points. Cells that were collected on days 3, 5, and 7 behaved more similarly to each other, although separation between these later time points was still evident across PC1 (Fig. 3). Although not as sharp a delineation, PC2 seemed to contribute to separation of the experimental samples by treatment condition. In general, cells that were untreated or those that were treated with the blank and low Dex microparticles behaved similarly to each other, while cells treated with the high Dex microparticles and free Dex behaved similarly and clustered together along the higher values on the PC2 spectrum.

Inflammatory gene analysis trends. Five genes related to macrophage inflammation were assessed over time and treatment condition. Importantly, cells that were treated with high Dex microparticles modulated inflammatory gene transcription in a manner similar to the free Dex group. Most of the anti-inflammatory effects of the treatment condition were apparent on day 1. Inflammatory gene expression at

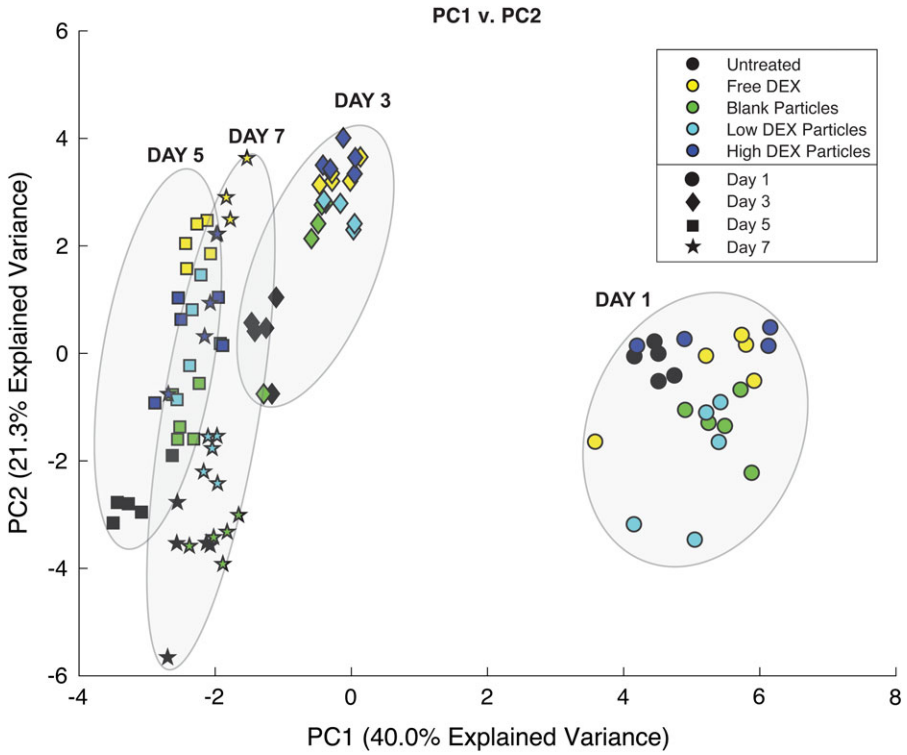

FIGURE 3. Principle component analysis of normalized gene expression data. Principle component 1 (PC1) and principle component 2 (PC2) were plotted against each other to visualize variability from the data set. Principle component 1 accounted for 40.0% of the data set's variance while principle component 2 accounted for 21.3% of the data set's variance.

later time points did not differ from the untreated controls, with all groups clearly decreasing inflammatory gene expression over time (Fig. 4).

TNF, the gene that encodes the potent proinflammatory cytokine tumor necrosis factor alpha,[11,13] exhibited different expression levels across treatment condition at day 1 (Fig. 4A,B). Untreated cells expressed *TNF* levels similarly to cells treated with blank microparticles. However, cells treated with high Dex microparticles expressed significantly lower levels of *TNF* compared to cells treated with blank microparticles and untreated controls. Furthermore, cells treated with high Dex microparticles acted similarly to positive control cells that were treated with continuous free Dex (Fig. 4B). Expression of *IL1B*, which encodes interleukin-1-beta, followed similar trends (Fig. 4C,D). Together these results suggest that intracellular Dex microparticles were able to modulate inflammatory gene expression in macrophages.

Homing gene analysis trends. Six genes related to monocyte-derived macrophage homing were assessed over time and treatment condition. Interestingly, Dex-loaded microparticles increased expression of homing genes in a similar manner to positive control cells treated with continuous free Dex. Furthermore, in some of the genes the effects on gene expression was maintained 7 days after microparticle administration. For example, *CCR1*, a gene associated with recruitment into or within inflamed tissue,[30] exhibited very different expression levels across conditions at day 7 (Fig. 5B,C). Low and high Dex microparticles seemed to exhibit a dose-dependent increase of *CCR1* expression relative to untreated controls. Also, high Dex microparticles behaved similarly to positive control cells continuously treated with free Dex (Fig. 5C).

CXCR4, a factor that leads to monocyte recruitment into tissues,[31] was differentially expressed across treatment conditions in macrophages on day 1. Cells loaded with high Dex microparticles significantly upregulated *CXCR4* expression to levels comparable to the positive control cells treated with continuous free Dex (Fig. 5F). *CCR2*, a gene that generates a protein associated with monocytes homing to injured or inflamed tissue,[14] was upregulated in the positive control cells treated with free Dex but not in the other treatment groups (Fig. 5I).

Interestingly, expression trends over time were dissimilar between homing genes. The genes *ITGB2* and *PECAM1* generally exhibited an increase in gene expression over time regardless of the treatment condition. The genes *CXCR4* and *ITGB1* generally exhibited a decrease in gene expression over time regardless of the treatment condition. The gene *CCR2* seemed to peak in expression on day 3 regardless of treatment condition. The gene *CCR1* exhibited variable expression trends over time depending on the treatment condition. Importantly, cells treated with high Dex microparticles exhibited expression trends mimetic of cells treated with continuous free Dex, suggesting that homing gene temporal regulation is complex but the high Dex microparticles generated the expected effects. For example, *CCR1* expression on day 1 and *ITGB2* expression on day 7 showed reduced gene expression in cells treated with high Dex microparticles and cells treated with continuous free Dex (Fig. 5A,B). These data

suggest that intracellular Dex microparticles are able to modulate the expression levels of some homing genes in macrophages up to 1 week after microparticle administration.

Phagocytosis gene analysis trends. Seven genes related to monocyte-derived macrophage phagocytosis were assessed over time and treatment condition (Fig. 6). Again, we observed that cells treated with high Dex microparticles acted similarly to the positive control cells treated with continuous Dex, even 7 days after microparticle administration. *CD163*, a gene associated with hemoglobin and haptoglobin scavenging,[15–18] and *MERTK*, a gene associated with apoptotic cell clearance,[17,18,20] were differentially expressed across treatment conditions in macrophages on day 7. As expected, free Dex treatment increased the expression of *CD163* and *MERTK*. However, cells treated with high Dex microparticles exhibited the same effect as the positive control cells (Fig. 6B, D).

Interestingly, expression trends over time were different for different genes. The genes *CD163* and *MFGE8* generally exhibited a decrease in gene expression over time regardless of the treatment condition. The gene *CD206* seemed to peak in expression on day 3 regardless of treatment condition. The genes *MERTK*, *PPARG*, *GAS6*, and *MARCO* exhibited variable expression trends over time depending on the treatment condition. Together, these results suggest that intracellular Dex microparticles are able to modulate gene expression related to phagocytosis in macrophages for 7 days after microparticle administration.

Iron metabolism gene analysis trends. Three genes related to monocyte-derived macrophage iron metabolism were assessed over time and treatment condition (Fig. 7). Expression trends over time were different across genes. The genes *HIF1A* and *FTH* generally exhibited a decrease in gene expression between days 1 and 5 regardless of the treatment condition. The gene *HEPH* exhibited variable expression trends over time depending on the treatment condition.

HIF1A, a gene that plays a central role in how iron regulates macrophage phenotype and iron metabolism,[32] exhibited different expression levels across conditions at day 1 (Fig. 7B). Cells treated with free Dex and cells treated with high Dex microparticles did not change *HIF1A* gene expression levels relative to untreated controls. However, cells treated with blank microparticles and cells treated with low Dex microparticles exhibited reduced *HIF1A* gene expression relative to untreated controls (Fig. 7B).

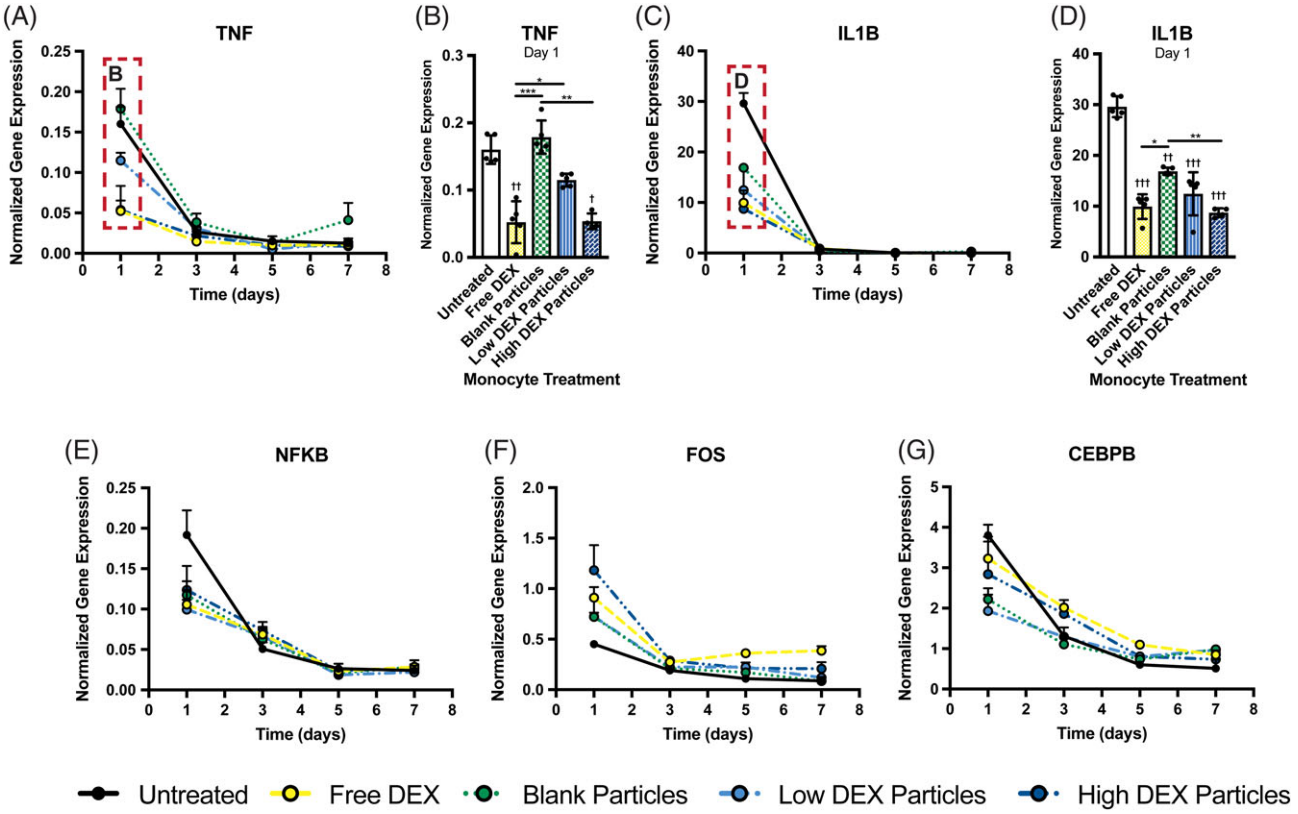

FIGURE 4. Gene expression over time of genes related to inflammation. All genes related to inflammation that were characterized decreased over time in the macrophage populations. Select timepoints, boxed in red, were graphed in a call-out box in order to visualize the effect of treatment condition (B, D). Plotted data represents the mean ± standard deviation of the data prior to transformation. All statistical tests were completed on transformed data. A one-way ANOVA investigating the effect of treatment condition was employed for select timepoints on a few genes (B, D). Tukey's Honest Significant Different post hoc test with correction for multiple comparisons was completed. *Denotes significant difference of $p < 0.05$; **denotes significant difference of $p < 0.01$; ***denotes significant difference of $p < 0.001$; and †denotes significant difference relative to untreated controls.

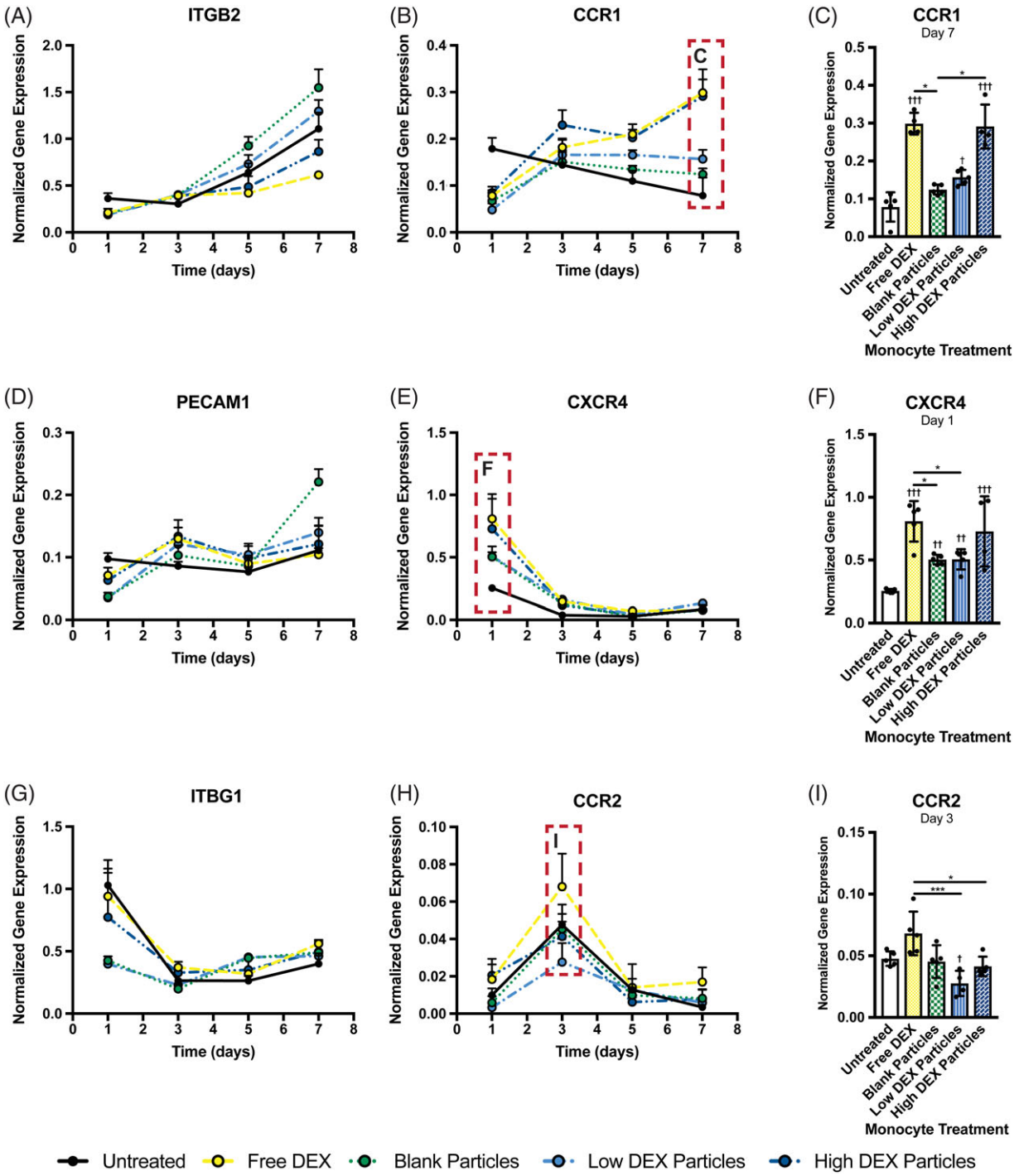

FIGURE 5. Gene expression over time of genes related to homing. Select timepoints, boxed in red, were graphed in a call-out box in order to visualize the effect of treatment condition (C, F, I). Plotted data represent the mean ± standard deviation of the data prior to transformation. All statistical tests were completed on transformed data. A one-way ANOVA investigating the effect of treatment condition was employed for select timepoints on a few genes (C, F, I). Tukey's Honest significant different post hoc test with correction for multiple comparisons was completed. *Denotes significant difference of $p < 0.05$; **denotes significant difference of $p < 0.01$; ***denotes significant difference of $p < 0.001$; and †denotes significant difference relative to untreated controls.

FTH, a gene associated with intracellular iron storage,[32] expressed differential gene expression in some cells treated with microparticles on day 7. Specifically, *FTH* expression was increased in cells treated with microparticles but microparticle loading with Dex inversely correlated with *FTH* transcription (Fig. 7D). Finally, *HEPH*, a gene associated with iron oxidation,[32] was not differentially regulated across treatment conditions on day 3 (Fig. 7F).

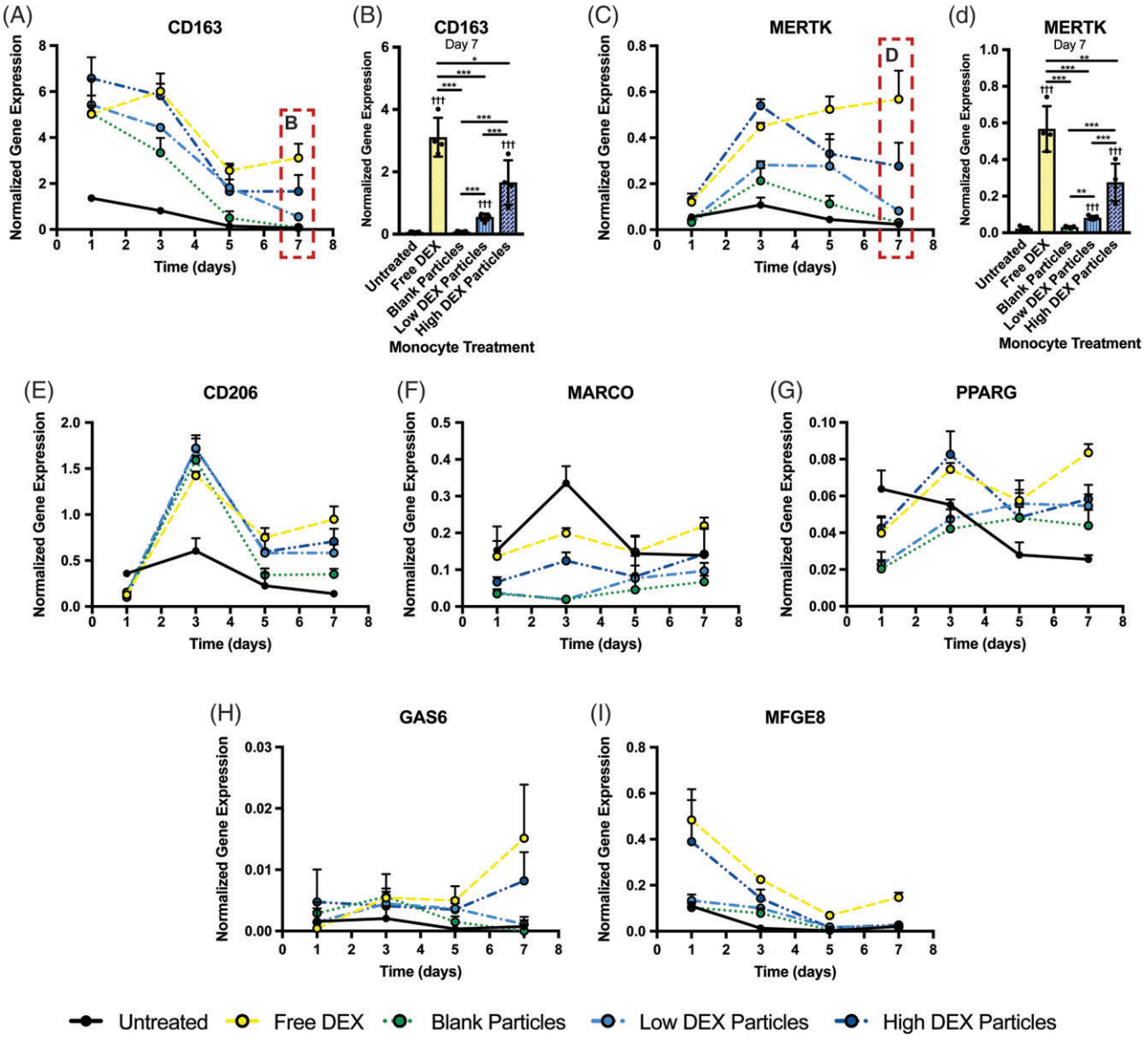

FIGURE 6. Gene expression over time of genes related to phagocytosis. Phagocytosis genes exhibited different trends in expression over time and over condition. Select timepoints, boxed in red, were graphed in a call-out box in order to visualize the effect of treatment condition (B, D). Plotted data represents the mean ± standard deviation of the data prior to transformation. All statistical tests were completed on transformed data. A one-way ANOVA investigating the effect of treatment condition was employed for select timepoints on a few genes (B, D). Tukey's Honest significant different post hoc test with correction for multiple comparisons was completed. *Denotes significant difference of $p < 0.05$; **denotes significant difference of $p < 0.01$; ***denotes significant difference of $p < 0.001$; and †denotes significant difference relative to untreated controls.

DISCUSSION

The immune system plays a major role in regulating pathology and tissue regeneration. Many researchers have attempted to harness the immune system through administration of immunomodulatory drugs or through biomaterial applications.[9,33–36] Several landmark studies showed the possibility of using biomaterials to modulate macrophage phenotype and behavior for therapeutic applications.[18,37–40] Here, we describe a novel strategy to use intracellular drug-loaded microparticles to modulate macrophage gene expression for up to 7 days after microparticle administration. Importantly, we found that gene expression related to inflammation can be mitigated when human primary monocytes are loaded with Dex-loaded microparticles. Furthermore, these microparticles enhanced gene expression related to wound healing behaviors such as homing and phagocytosis for up to 7 days *in vitro*. Diminishing inflammatory behaviors of macrophages while enhancing the expression of homing and phagocytosis behaviors may facilitate an enriched wound healing phenotype for tissue regeneration. These data suggest that loading monocyte-derived macrophages with intracellular microparticles could be a novel mechanism to modulate macrophage behaviors in a cell-specific, persistent manner. Exogenously loading monocyte-derived macrophages with drug-loaded biomaterials has vast implications in wound repair and tissue regeneration research. Instead of fabricating biomaterials with influence over the cells in a particular area,[41,42]

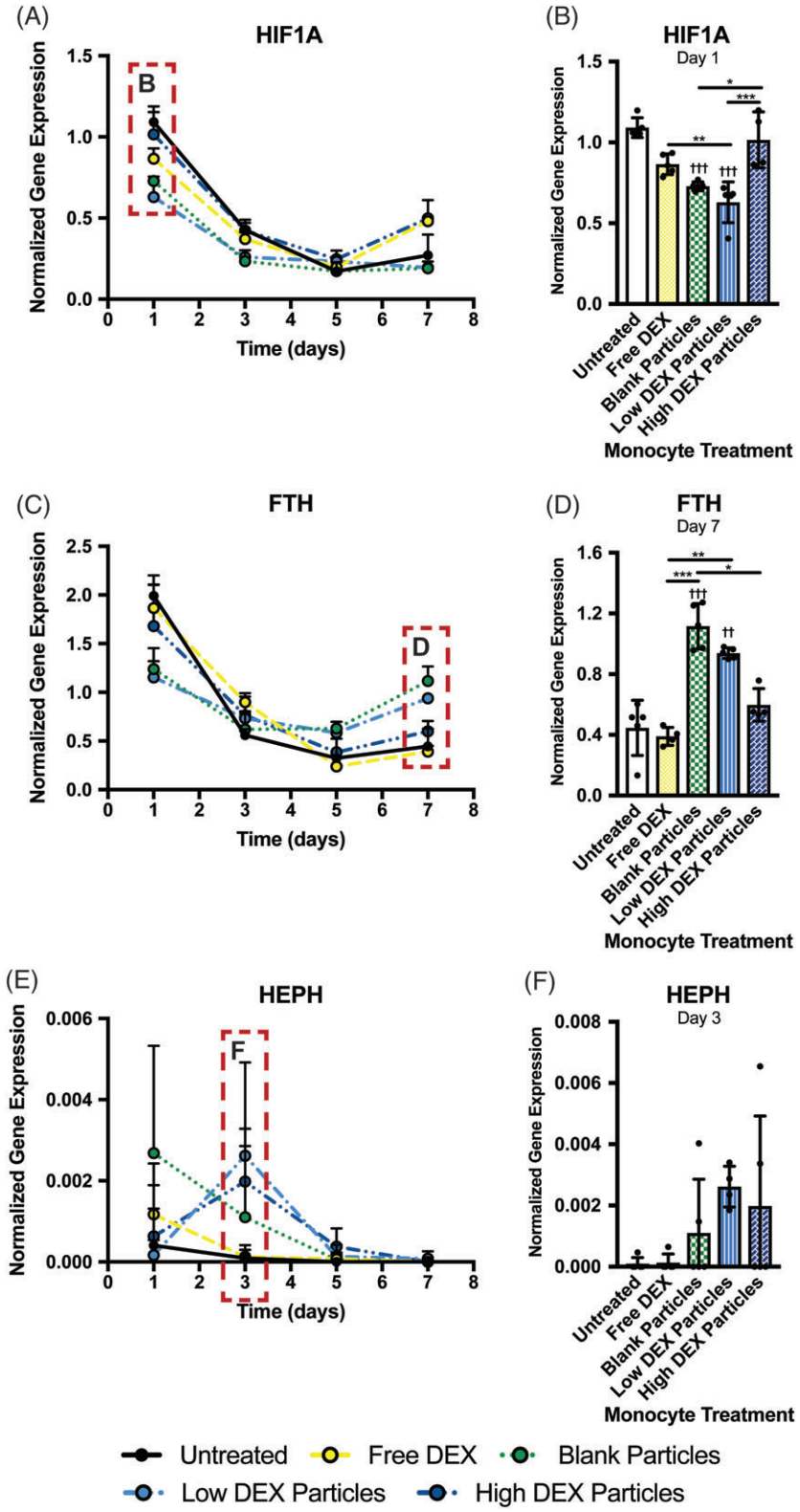

FIGURE 7. Gene expression over time in genes related to iron metabolism. Iron metabolism genes generally decrease over time. Select timepoints, boxed in red, were graphed in a call-out box in order to visualize the effect of treatment condition (B, D, F). All statistical tests were completed on transformed data. A one-way ANOVA investigating the effect of treatment condition was employed for select timepoints on a few genes (B, D, F). Tukey's Honest significant different post hoc test with correction for multiple comparisons was completed. *Denotes significant difference of $p < 0.05$; **denotes significant difference of $p < 0.01$; ***denotes significant difference of $p < 0.001$; and †denotes significant difference relative to untreated controls.

intracellular microparticles could have cell-specific resolution within the body. Within this study, we exogenously loaded monocyte-derived macrophages with Dex microparticles to selectively deliver therapeutics to these specific cells. This immunomodulatory strategy could have therapeutic applications in a multitude of difficult-to-access inflammatory pathologies including traumatic brain injury,[47,48] myocardial infarction,[49] or diabetes.[50]

The effects of Dex on macrophage behavior likely result from intracellular release of Dex from the microparticles, although the mechanism of this process and the temporal effects on gene expression require further investigation. Interestingly, all the inflammatory genes we investigated decreased in gene expression over time, although the decreases were more pronounced for treatments that contained Dex. This general trend may suggest that the transition from monocytes to macrophages reduces inflammation when the cells are in non-inflammatory conditions. Future studies aimed to characterize cell transcription of these genes in a pro-inflammatory environment are required to determine if these treatments can preclude inflammatory polarization in environments that are more representative of damaged tissue.

We also observed that cells treated with blank microparticles exhibited several significant changes in gene expression relative to untreated controls across multiple timepoints. These data suggest that microparticle administration without the aid of drug can drastically affect cell gene expression. However, we cannot determine if the results observed were induced by the process of phagocytosis or were induced by the storage of intracellular microparticles. Further characterization of the effects of the vast array of established microparticle formulations on macrophages could provide useful information about how to modulate macrophage behavior without pharmacological intervention.[34,43]

Global gene expression mapping through the dendrogram and PCA suggested that there was a notable distinction between gene expression on day 1 and gene expression at later timepoints. We suspect that this finding may result from a large impact of the monocyte-to-macrophage differentiation process that affects gene expression, especially because the negative and positive control cells (untreated or treated with continuous free Dex) clustered with the other treatment conditions over time. However, the initial exposure of the foreign biomaterials to cells could also play an important role in the cell changes over time.[44]

Surprisingly, while cells treated with high Dex microparticles acted in a similar way to positive control cells treated with continuous free Dex, these two groups did not always increase homing, phagocytosis, or iron metabolism gene expression as we expected. Within the six homing genes, seven phagocytosis genes, and three iron metabolism genes we investigated, we observed increasing, decreasing, and unchanging trends of gene expression over time. Cells with Dex treatments (in free Dex and in high Dex microparticle conditions) seemed to act similarly to each other by enhancing some but not all of these genes. We suspect that these genes could have exhibited unique expression patterns over time because homing, phagocytosis, and metabolism functions are complex and may require temporal resolution to best execute these behaviors.

While the results of this study suggest that drug-loaded microparticles can modulate macrophage phenotype intracellularly, this study did have some limitations. First, this study utilized monocytes derived from one human donor. While clustering of experimental replicates was notable – suggesting that independent variables contributed to trends more than random variation – it cannot be dismissed that human donor-to-donor variability could affect these trends. In our experience, human monocytes from different donors typically exhibit the same response trends but can display large differences in the magnitude of the response.[45] A second limitation of this study is that we exclusively characterized gene expression as a metric of change in macrophage phenotype. While researchers have found that gene expression is a very reliable indicator of macrophage phenotype,[46] these results will need to be validated on a functional level in future studies. Finally, as previously mentioned, the results will need to be confirmed in the presence of inflammatory challenge to more closely mimic the intended clinical applications. *In vivo* environments are often complex, and these results will need validation in appropriate preclinical models of tissue injury and healing.

In summary, we found that exogenously loading monocytes with drug-loaded microparticles could modulate their behavior up to 7 days after microparticle administration. We believe that cultivating a more comprehensive understanding of macrophage–biomaterial interactions will inform the development of translational, immunomodulatory treatment options that could target a number of inflammatory diseases and disorders.

ACKNOWLEDGMENTS

This work was supported by the Department of Veteran's Affairs (RR&D Merit Review #I01-RX001097 to DKC); the NIH/NHLBI (R01-HL130037 to KLS); and the Department of Education GAANN iCARE Fellowship (to KLW).

REFERENCES

1. Spiller KL, Koh TJ. Macrophage-based therapeutic strategies in regenerative medicine. Adv Drug Deliv Rev 2017;122:74–83.
2. Wang G, Zhang J, Hu X, Zhang L, Mao L, Jiang X, Liou AK-F, Leak RK, Gao Y, Chen J. Microglia/macrophage polarization dynamics in white matter after traumatic brain injury. J Cereb Blood Flow Metab 2013;33:1864–1874.
3. Wynn TA, Chawla A, Pollard JW. Macrophage biology in development, homeostasis and disease. Nature 2013;496:445–455.
4. Novak ML, Koh TJ. Phenotypic transitions of macrophages orchestrate tissue repair. Am J Pathol 2013;183:1352–1363.
5. Mosser DM, Edwards JP. Exploring the full spectrum of macrophage activation. Nat Rev Immunol 2008;8:958–969.
6. Spiller KL, Anfang RR, Spiller KJ, Ng J, Nakazawa KR, Daulton JW, Vunjak-Novakovic G. The role of macrophage phenotype in vascularization of tissue engineering scaffolds. Biomaterials 2014;35:4477–4488.
7. Graney PL, Lurier EB, Spiller KL. Biomaterials and bioactive factor delivery Systems for the Control of macrophage activation in regenerative medicine. ACS Biomater Sci Eng 2018;4:1137–1148.
8. Spiller KL, Nassiri S, Witherel CE, Anfang RR, Ng J, Nakazawa KR, Yu T, Vunjak-Novakovic G. Sequential delivery of immunomodulatory

cytokines to facilitate the M1-to-M2 transition of macrophages and enhance vascularization of bone scaffolds. Biomaterials 2015;37: 194–207.
9. Lee S, Kivimäe S, Dolor A, Szoka FC. Macrophage-based cell therapies: The long and winding road. J Control Release 2016;240: 527–540.
10. Kigerl KA, Gensel JC, Ankeny DP, Alexander JK, Donnelly DJ, Popovich PG. Identification of two distinct macrophage subsets with divergent effects causing either neurotoxicity or regeneration in the injured mouse spinal cord. J Neurosci 2009;29:13435–13444.
11. David S, Kroner A. Repertoire of microglial and macrophage responses after spinal cord injury. Nat Rev Neurosci 2011;12: 388–399.
12. Pentecost AE, Lurier EB, Spiller KL. Nanoparticulate systems for controlling monocyte/macrophage behavior. Microscale Technologies for Cell Engineering. Springer, Cham, 2016;291–304.
13. van der Goes A, Hoekstra K, van den Berg TK, Dijkstra CD. Dexamethasone promotes phagocytosis and bacterial killing by human monocytes/macrophages in vitro. J Leukoc Biol 2017;67: 801–807.
14. Penton-Rol G, Cota M, Polentarutti N, Luini W, Bernasconi S, Borsatti A, Sica A, LaRosa GJ, Sozzani S, Poli G, Mantovani A. Up-regulation of CCR2 chemokine receptor expression and increased susceptibility to the multitropic HIV strain 89.6 in monocytes exposed to glucocorticoid hormones. J Immunol 1999;163: 3524–3529.
15. Schaer DJ, Boretti FS, Schoedon G, Schaffner A. Induction of the CD163-dependent haemoglobin uptake by macrophages as a novel anti-inflammatory action of glucocorticoids. Br J Haematol 2002; 119:239–243.
16. Gratchev A, Kzhyshkowska J, Utikal J, Goerdt S. Interleukin 4 and dexamethasone counterregulate extracellular matrix remodelling and phagocytosis in type 2 macrophages. Scand J Immunol 2005; 61:10–17.
17. Zizzo G, Hilliard BA, Monestier M, Cohen PL. Efficient clearance of early apoptotic cells by human macrophages requires M2c polarization and MerTK induction. J Immunol 2012;189:3508–3520.
18. Pentecost AE, Gogotsi Y, Spiller KL. Anti-inflammatory effects of octadecylamine-functionalized nanodiamond on primary human macrophages. Biomater Sci 2017;5:2131–2143.
19. Buechler C, Ritter M, Orsó E, Langmann T, Klucken J, Schmitz G. Regulation of scavenger receptor CD163 expression in human monocytes and macrophages by pro- and antiinflammatory stimuli. J Leukoc Biol 2000;67:97–103.
20. Ehrchen J, Steinmüller L, Barczyk K, Tenbrock K, Nacken W, Eisenacher M, Nordhues U, Sorg C, Sunderkötter C, Roth J. Glucocorticoids induce differentiation of a specifically activated, anti-inflammatory subtype of human monocytes. Blood 2007;109: 1265–1274.
21. Vettori A, Greenald D, Wilson GK, Peron M, Facchinello N, Markham E, Sinnakaruppan M, Matthews LC, McKeating JA, Argenton F, van Eeden FJM. Glucocorticoids promote Von Hippel Lindau degradation and Hif-1α stabilization. Proc Natl Acad Sci USA 2017;114:9948–9953.
22. Advani S, Lafrancis D, Bogdanovic E, Taxel P, Raisz LG, Kream BE. Dexamethasone suppresses in vivo levels of bone collagen synthesis in neonatal mice. Bone 1997;20:41–46.
23. Cooper PR, Moody S, Clark WK, Kirkpatrick J, Maravilla K, Gould AL, Drane W. Dexamethasone and severe head injury. J Neurosurg 1979;51:307–316.
24. Duffy BA, Chun KP, Ma D, Lythgoe MF, Scott RC. Dexamethasone exacerbates cerebral edema and brain injury following lithium-pilocarpine induced status epilepticus. Neurobiol Dis 2014;63:229–236.
25. Braakman R, Schouten HJ, Blaauw-van Dishoeck M, Minderhoud JM. Megadose steroids in severe head injury. Results of a prospective double-blind clinical trial. J Neurosurg 1983;58:326–330.
26. Kunicka JE, Talle MA, Denhardt GH, Brown M, Prince LA, Goldstein G. Immunosuppression by glucocorticoids: Inhibition of production of multiple lymphokines by in vivo administration of dexamethasone. Cell Immunol 1993;149:39–49.
27. Giles AJ, Hutchinson MKND, Sonnemann HM, Jung J, Fecci PE, Ratnam NM, Zhang W, Song H, Bailey R, Davis D, Reid CM, Park DM, Gilbert MR. Dexamethasone-induced immunosuppression: Mechanisms and implications for immunotherapy. J Immunother Cancer J ImmunoTher Cancer 2018;6:1–13.
28. Xing K, Gu B, Zhang P, Wu X. Dexamethasone enhances programmed cell death 1 (PD-1) expression during T cell activation: An insight into the optimum application of glucocorticoids in anticancer therapy. BMC Immunol 2015;16:1–9.
29. Kubota Y, Takahashi S, Matsuoka O. Dependence on particle size in the phagocytosis of latex particles by rabbit alveolar macrophages cultured in vitro. J Toxicol Sci 1983;8:189–195.
30. Shi C, Pamer EG. Monocyte recruitment Suring infection and inflammation. Nat Rev Immunol 2014;11:762–774.
31. Caulfield J, Fernandez M, Snetkov V, Lee T, Hawrylowicz C. CXCR4 expression on monocytes is up-regulated by dexamethasone and is modulated by autologous CD3+T cells. Immunology 2002;105:155–162.
32. Nairz M, Theurl I, Swirski FK, Weiss G. "Pumping iron"—How macrophages handle iron at the systemic, microenvironmental, and cellular levels. Eur J Physiol 2017;469:397–418.
33. Jiang K, Weaver JD, Li Y, Chen X, Liang J, Stabler CL. Biomaterials local release of dexamethasone from macroporous scaffolds accelerates islet transplant engraftment by promotion of anti-inflammatory M2 macrophages. Biomaterials 2017;114:71–81.
34. Vegas AJ, Veiseh O, Doloff JC, Ma M, Tam HH, Bratlie K, Li J, Bader AR, Langan E, Olejnik K, Fenton P, Kang JW, Hollister-Locke J, Bochenek MA, Chiu A, Siebert S, Tang K, Jhunjhunwala S, Aresta-Dasilva S, Dholakia N, Thakrar R, Vietti T, Chen M, Cohen J, Siniakowicz K, Qi M, McGarrigle J, Lyle S, Harlan DM, Greiner DL, Oberholzer J, Weir GC, Langer R, Anderson DG. Combinatorial hydrogel library enables identification of materials that mitigate the foreign body response in primates. Nat Biotechnol 2016;34:345–352.
35. Franz S, Rammelt S, Scharnweber D, Simon JC. Immune responses to implants - a review of the implications for the design of immunomodulatory biomaterials. Biomaterials 2011;32:6692–6709.
36. San Emeterio CL, Olingy CE, Chu Y, Botchwey EA. Selective recruitment of non-classical monocytes promotes skeletal muscle repair. Biomaterials 2017;117:32–43.
37. Mitchell MJ, Wayne EC, Rana K, Schaffer CB, King MR. TRAIL-coated leukocytes that kill cancer cells in the circulation. Proc Natl Acad Sci USA 2014;111:930–935.
38. Yu SS, Lau CM, Barham WJ, Onishko HM, Nelson CE, Li H, Smith CA, Yull FE, Duvall CL, Giorgio TD. Macrophage-specific RNA interference targeting via "click", mannosylated polymeric micelles. Mol Pharm 2013;10:975–987.
39. Das A, Segar CE, Hughley BB, Bowers DT, Botchwey EA. The promotion of mandibular defect healing by the targeting of S1P receptors and the recruitment of alternatively activated macrophages. Biomaterials 2013;34:9853–9862.
40. Wang Y, Lin YX, Qiao SL, An HW, Ma Y, Qiao ZY, Rajapaksha RPYJ, Wang H. Polymeric nanoparticles enable reversing macrophage in tumor microenvironment for immunotherapy. Biomaterials 2017; 112:153–163.
41. Purcell BP, Lobb D, Charati MB, Dorsey SM, Wade RJ, Zellars KN, Doviak H, Pettaway S, Logdon CB, Shuman J a, Freels PD, Gorman Iii JH, Gorman RC, Spinale FG, Burdick JA. Injectable and bioresponsive hydrogels for on-demand matrix metalloproteinase inhibition. Nat Mater 2014;13:653–661.
42. Zhang X, Li Y, Chen YE, Chen J, Ma PX. Cell-free 3D scaffold with two-stage delivery of miRNA-26a to regenerate critical-sized bone defects. Nat Commun 2016;7:10376.
43. Akilbekova D, Philiph R, Graham A, Bratlie KM. Macrophage reprogramming: Influence of latex beads with various functional groups on macrophage phenotype and phagocytic uptake in vitro. J Biomed Mater Res Part A 2015;103:262–268.
44. Xia Z, Triffitt JT. A review on macrophage responses to biomaterials. Biomed Mater 2006;1:R1–R9.
45. Witherel CE, Graney PL, Freytes DO, Weingarten MS, Spiller KL. Response of human macrophages to wound matrices in vitro. Wound Repair Regen 2016;24:514–524.
46. Xue J, Schmidt SV, Sander J, Draffehn A, Krebs W, Quester I, DeNardo D, Gohel TD, Emde M, Schmidleithner L, Ganesan H, Nino-Castro A, Mallmann MR, Labzin L, Theis H, Kraut M, Beyer M, Latz E, Freeman TC, Ulas T, Schultze JL. Transcriptome-based network analysis reveals a spectrum model of human macrophage activation. Immunity 2014;40:274–288.

47. Cullen DK, Harris JP, Browne KD, Wolf JA, Duda JE, Meaney DF, Margulies SS, Smith DH. A porcine model of traumatic brain injury via head rotational acceleration. Methods Mol Biol 2016;1462: 289–324.
48. Wofford KL, Harris JP, Browne KD, Brown DP, Grovola MR, Mietus CJ, Wolf JA, Duda JE, Putt ME, Spiller KL, Kacy Cullen D, Grovolaa MR, Mietus CJ, Wolf JA, Duda JE, Putt ME, Spiller KL, Cullen DK, Grovola MR, Mietus CJ, Wolf JA, Duda JE, Putt ME, Spiller KL, Kacy Cullen D. Rapid neuroinflammatory response localized to injured neurons after diffuse traumatic brain injury in swine. Exp Neurol 2017;290:85–94.
49. Herdrich BJ, Danzer E, Davey MG, Englefield V, Gorman JH, Gorman RC, Liechty KW. Regenerative healing following fetal myocardial infarction. Eur J Cardiothorac Surg 2010;38:691–698.
50. Eizirik DL, Colli ML, Ortis F. The role of inflammation in insulitis and b-cell loss in type 1 diabetes. Nat Rev Endocrinol 2009;5:219–226.